

Cite this: DOI: 10.1039/c0xx00000x

www.rsc.org/xxxxxx

SUPPORTING INFORMATION

Bioconjugated Silicon Quantum Dots from One-Step Green Synthesis

Romuald Intartaglia,^{*[a](#)} Annette Barchanski,^b Komal Bagga,^a Alessandro Genovese,^c Gobind Das,^e Philipp Wagener,^d Enzo Di Fabrizio,^e Alberto Diaspro,^a Fernando Brandi,^a and Stephan Barcikowski^d

Received 16th November 2011, Accepted 27th December 2011

DOI: 10.1039/c2nr11763k

Synthesis of bioconjugated Si dots :

Laser generation of bioconjugated Si-NPs was carried out using a femtosecond laser system (Spitfire Pro, Spectra-Physics) delivering 120 fs laser pulses with a wavelength of 800 nm at a repetition rate of 5 kHz (maximum energy: 500 μJ per pulse). A lens with focal length of 40 mm was used. The pulse energy (100 μJ) and a focal position of - 4 mm respect to the target surface were chosen for the efficient Si-NPs generation³⁰ and to preserve the integrity³⁷ and functionality⁴² of SSO biomolecule. The target material (99.999 % Si from Alpha Aesar) in the form of a cylinder with diameter of 6 mm and thickness of 10 mm, was placed on the bottom of a Petri dish filled with 800 μL of a 1 μM aqueous solution of SSO (H₂O : >18 MΩ cm, SSO : 5' GGCGACTGTGCAAGCAGA3'-SH). The 18-mer single-stranded oligonucleotides biomolecule were purchased from Purimex (D-34393 Grebenstein, sequence 5' GGC-GAC-TGT-GCA-AGC-AGA 3') with a C12-thiol 3' modification. The thickness of the liquid layer above the target was 1 mm. The target was placed on an x-y motorized stage, that moved at constant speed of 1 mm s⁻¹ in a spiral with outer radius of 1 mm and an inner radius of 0.4 mm. time of irradiation was fixed (180 s).

Sample characterisations:

UV/vis absorption measurements of the colloidal solution were recorded in the spectral region 190-1100 nm, using a cary 6000 UV-VIS double beam spectrophotometer. The photoluminescence (PL) measurements for colloidal solution were carried out in the 350-600 nm wavelength range by Fluoroma-4 Spectrofluorometer (JobinYvon-Horiba) fitted with a photomultiplier and a Xenon lamp source. PL and absorption spectra were corrected for solvent contribution. Zeta potential and hydrodynamic size measurements of Si-NPs were performed by dynamic light scattering with the Zetasizer ZS (Malvern Instruments). The solutions were diluted 1:10 and the resulting dilution was injected into the electrophoretic cell. The average value of three consecutive measurements was taken for documentation.

SSO-bioconjugated Si-NPs solution was deposited directly onto carbon-coated 300 mesh copper grid and leaving the solution to evaporate. The conventional Transmission electron

microscopy (TEM) imaging was performed with a JEOL Jem 1011 microscope working at an acceleration voltage of 100KeV.

High angular annular dark field (HAADF) measurements via scanning TEM (STEM) mode were performed with a JEOL JEM-2200FS microscope, equipped with a field emission gun working at an accelerating voltage of 200 kV, a CEOS spherical aberration corrector of objective lens and an "in-column" Omega filter, and using a camera length of 50 cm and a probe size of 0.7 nm. The chemical composition of bio-functionalized particles was determined by energy dispersive x-ray spectroscopy (EDS) analysis performed in STEM mode, with a JED-2300 Si(Li) detector.

Raman scattering measurements were performed by Renishaw inVia microscopy. Microprobe Raman spectra were excited by 633 nm laser line in backscattering geometry through a 100X objective (NA= 0.9) with the laser power fixed to 1.5 mW and the accumulation time 20 sec. The experimental set-up consists of a grating 1800 lines/mm with spectral resolution of about 1.1 cm⁻¹. The sample was deposited by a drop coating deposition (DCD) technique, in which the substance was dropped over the CaF₂ substrate and waited for evaporation of excess liquid. The evaporation of liquid water leads to the formation of coffee ring.

Various measurements were performed at different locations in order to have clear picture of the sample content. All the SERS spectra were, firstly, baseline-corrected using maximum 3rd order polynomial with the help of WiRE 3.0 and then normalized to 1.

Evaluation of surface coverage of Si dots with SSO ligand:

The determination of conjugation between biomolecules and silicon nanoparticles has been evaluated by ultracentrifugation and optical experiments. In a first step, reference solution was centrifuged at different RCF to define optimal parameter for total removal of Si NP in the supernatant. This could be achieved at 44.700 RCF (data not shown), while all analyzed biomolecules were found in prior tests to sediment not until a speed of 400.000 RCF is reached. Therefore, 400 μL of bioconjugate samples were centrifuged at 44.700 RCF. Supernatant containing unbound biomolecules was transferred into a blank glass vessel for later UV-Vis analysis, while bioconjugates containing pellet was taken up in 200 μL double distilled Water (ddH₂O) and washed by two additional centrifugation steps at 44.700 RCF. Supernatants of washing steps were added to supernatant of first centrifugation

step and pellet was finally taken up in 100 μ L ddH₂O and stored in another glass vessel. Supernatant of three centrifugation steps as well as bioconjugates containing pellet of the third centrifugation were analyzed terminally by UV-Vis spectroscopy.
5 The results are reported in Table 1S. The surface coverage of Si-NPs with SSO ligands was calculated referring to a protocol of our last report⁴⁴, using distinct parameters of the Si-NPs like their average size, density, mass and manually calculated surface area. The number of nanoparticle were calculated based on NPs
10 average diameter estimated from TEM analysis (Figure 1b) and NP concentration estimated from Inductively Coupled Plasma Optical Emission Spectrometry measurements of the conjugated Si-NPs, 3.5 nm and 4.15 μ g/mL, respectively. Based on the determined 20 % conjugation efficiency of SSO to Si-NP surface,
15 number of attached SSO molecules and amount of substance was calculated and set in ratio to total Si-NPs number as well as total surface area of nanoparticles in solution. Thus, a surface coverage of 66 pmol/cm² was identified, corresponding to 1.5 SSO molecules loaded to a single Si nanoparticle in average.

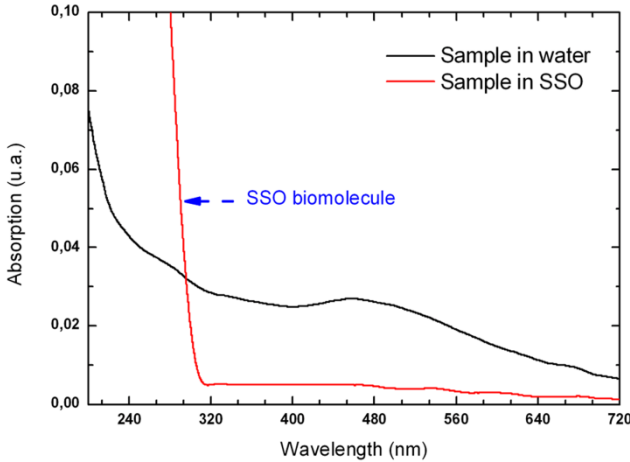
20

Measurement of the fluorescence quantum yield:

The quantum yield (Q.Y.) of the SI-SSO bioconjugated NPs were determined by comparison with a standard of known Q.Y. (freshly prepared solution of Alexa 405 in deionized water; Q.Y. 25 54%), using the following formula: $\Phi_{NP} = \Phi_{Standard} (gradNP/gradStandard)(nNP^2/nStandard^2)$ with Φ being the Q.Y., grad the gradient (slope) of the plot of the integrated fluorescence intensity vs. absorbance and n the refractive index of the solvent (1.33 for deionized for both). Samples of SI-SSO bioconjugated 30 NPs in water were put into 1 cm quartz cuvettes and diluted until the absorbance was below 0.15. At least three samples of different concentration were prepared. The absorbance of the standard was adjusted to be equal to each NP dispersion at the excitation wavelength.

35

Experimental data:



40 Figure 1S : Absorption spectra of the unconjugated (black line) and conjugated Si-NPs (red line) produced via PLAL method at lower pulse energy in deionized water and SSO-biomolecule environment, respectively.

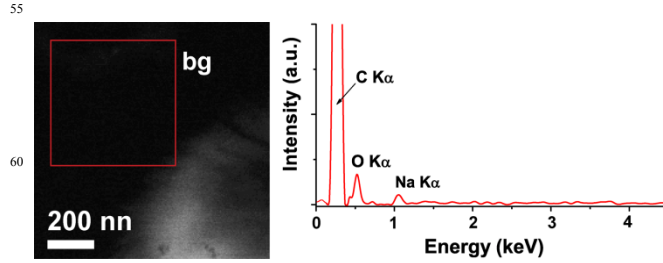
Table 1S: Analysis of SSO conjugation efficiency and Si-NP surface coverage after ultracentrifugation.
45

Biomolecule	Unbound Biomolecule	bound Biomolecule	Conjugation Efficiency [%]	Surface Coverage [pmol/cm ²]
SSO	0.8 μ M	0.2 μ M	20	66

Table 2S : Analytical analysis measurement by Inductively Coupled Plasma Optical Emission Spectrometry (ICP-OES) of deionized water used for PLAL experiments.
50

Element	Amount (ppm)	Standard deviation
Ca	0.0001	0.0002
K	0.0420	0.0009
Mg	0.0000	0.0001
Na	0.0270	0.0011

HAADF-STEM analysis



55 Figure 2S : HAADF-STEM image (left) of a representative background region (bg) without Si-NPs; red rectangle highlights the scanned area for the STEM-EDX elemental quantification (right); the corresponding STEM-EDX spectrum exhibited only the signals of C, O and Na elements. The absence of S-K α peaks confirms the absence of SSO-
70 biomolecule in the region. The C-K α , O-K α and Na-K α peaks are due to C-film of TEM grid and residuals of solution, respectively.

75

80

85

Optical properties of SiNPs prepared in deionized water

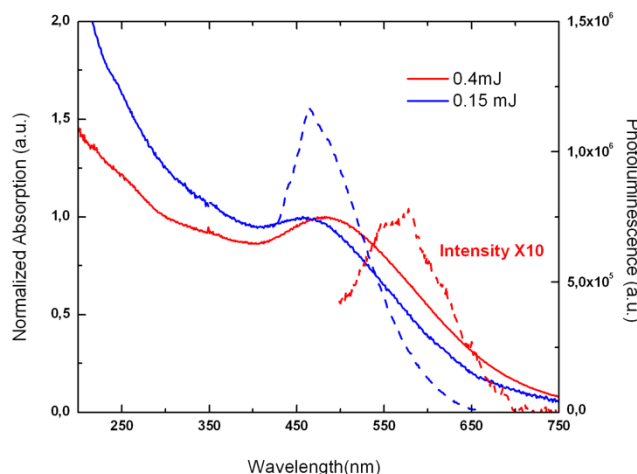


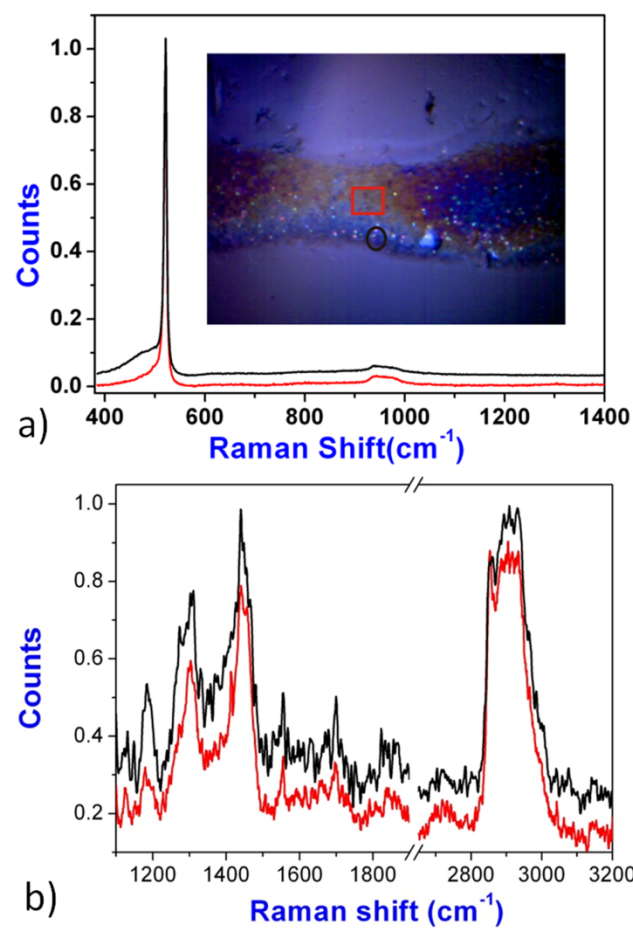
Figure 3S: Absorption and photoluminescence spectra of Si NPs produced via PLAL method in deionized water in two regime of laser power.

5

Raman analysis:

In order to understand the chemical/structural information, micro-probe Raman scattering was performed on the sample Si-NPs conjugated with biomolecules. The measurements were carried out in three different ranges; 380-1400 cm⁻¹ (low frequency range), and 1100-3200 cm⁻¹ (high frequency range) to evaluate Si-NPs related structural and chemical bonding of Si-NPs attached to DNA biomolecules, respectively. Drop-casted samples show a coffee ring with the molecular concentration varying from periphery to centre. Various measurements at different locations have been made. The optical image of coffee ring and the location where the measurements were performed is illustrated in the inset of Figure 4Sa. The color of the Raman spectra is correspondence to the color used in the covered area in the optical image. Two basic informations can be obtained just in first look of Raman spectra in Figure 4Sa and 4Sb; a) the presence of Si-NPs and the presence of biomolecules (i.e. DNA in this case). The sharp peak at around 520 cm⁻¹ with an asymmetry in low frequency side, in Figure 4Sa, confirms the presence of Si-NPs (Intartaglia et al, 2011, Mariotto et al, 2005, Daldosso et al, 2007). The deep analysis of the Raman bands at around 480 cm⁻¹ shows also the presence of SiOx which could be due the oxidation of Si-NPs during the abrupt cooling of nanoparticles in water environment. The deconvolution of Raman spectra (Fig. 4Sa) gives the presence of the different bands, centred at 480, 516 and 520 cm⁻¹ (Intartaglia et al, 2011). These bands provide informations regarding the presence of SiOx together with Si nanoparticle. In Figure 4b, Raman spectra in the range of 1200-3200 cm⁻¹ show various vibrational bands of inter/intra DNA molecules when it is attached to the Si-NPs (with very thin SiOx in the shell). There are various vibrational bands, centred at 1182, 1260, and 1305 cm⁻¹ which are related to the combination of thymine (T) and cytosine (C), the combination of adenine (A) and cytosine (C), and to the combination of adenine (A) and cytosine (C) nucleic acid bases, respectively (Ruiz-Chica et al. 2004). A shoulder peak at around 1277 cm⁻¹ is observed which could be related to the stretching vibration of Si-C/Si-CH

(in the configuration of H_xC_{4-x}-SiO_x, where x=1-3) (Das et al, 2006; Hai-wen Gu et al, 2004). This chemical bond, most probably, is formed while the ablation process in order to produce Si-NPs in the presence of biomolecules. As in the Figure 4Sa, a broad band at around 480 cm⁻¹ is observed which is from SiOx, we propose that the reaction with biomolecules is occurred on the defect site of this SiOx (x=1-3) layer (D. Knopp et al. 2009). In addition, various Raman bands, centred at around 1450, and the broad band at around 2900 cm⁻¹, are also found which are associated to the C-H bending and stretching vibrations, respectively (Ruiz-Chica et al. 2004).



55 Figure 4S : a) Optical image of coffee ring and the location where the measurements were performed is illustrated in inset. b) Raman analysis of the SSO-conjugated Si-NPs. Color of the Raman spectra corresponds to the color used in the covered area in the optical image.

60

Reference:

- R. Intartaglia, K. Bagga, F. Brandi, A. Genovese, E. Di Fabrizio and A. Diaspro, *J. Phys. Chem. C.*, 2011, **115**, 5102-5107.
G. Mariotto ,G. Das, A. Quaranta, G. Della Mea, F. Corni and R. Tonini, *J. Appl. Phys.*, 2005, **97**, 113502.
N. Daldosso, G. Das, S. Larcheri, G. Mariotto, G. Dalba, L. Pavesi, A. Irrera, F. Priolo, F. Iacona and F. Rocca *J. Appl. Phys.*, 2007, **101**, 113510.

- A.J. Ruiz-Chica, M.A. Medina, F. Sanchez-Jimenez, and F.J. Ramirez, *Nucleic Acids Research*, 2004, **32**, 579-589
- G. Das, G. Mariotto, and A. Quaranta, *J. Electrochemical Soc.*, 2006, **153**, F41-F51
- H.W. Gu, P. Xie, Z.R. Shen, D.Y. Shen, J.M. Zhang and R.B. Zhang, *Chin. J. Pol. Sci.*, 2004, **22**, 463-468.
- D. Knopp, D. Tang, R. Niessner, *Analytica Chimica Acta*, 2009, **647**, 14-30.